Research on Selective Oxidation of Carbon and Aluminum with Introduction of CO_2 in RH Refining of Low-Carbon Steel Process

BAOCHEN HAN, RONG ZHU, YIQIANG ZHU, RUNZAO LIU, WENHE WU, QIANG LI, and GUANGSHENG WEI

The injection of CO_2 during the Rheinstahl–Heraeus (RH) refining process as a lifting gas is a new attempt for the steel industry, and can promote refining effect and realize the utilization of CO_2 as a resource. In the present study, the thermodynamic equilibrium of the RH refining process through CO_2 injection instead of Ar was calculated using FactSage software. A selective oxidation sequence of [C] and [Al] with CO_2 was studied and analyzed under the RH refining temperature and vacuum degree. In addition, the oxidation zones of carbon and aluminum were both defined. Industrial trials were preliminarily conducted to verify the above theory. The results show that CO_2 has the potential to be used to refine low-carbon steel in RH, but its refining effect is affected by the [Al] content in steel. By reducing the additive amount of aluminum alloy in the ladle furnace and replenishing the aluminum during the late stage of the RH refining process, CO_2 injection can achieve a lower temperature drop of molten steel and a better refining effect than Ar during the RH degassing process.

https://doi.org/10.1007/s11663-018-1417-2

I. INTRODUCTION

AT present, the iron and steel industries still generate large amounts of CO_2 emissions. For the sustainable development of all steel industries, it is imperative that new technologies be found to reduce the CO_2 emissions or utilize CO_2 as a resource. In this connection, some scholars have studied the methods for cutting CO_2 emissions or applying CO_2 in resourceful manner. To recycle blast furnace gas, the ULCOS program in Europe was launched, which has achieved a CO_2 emissions reduction of 50 pct.[1–3] The COURSE50 program was promoted in Japan to decrease the CO_2 emissions by 30 pct using CO gas separation and recycling.[4] Some others have introduced CO_2 gas creatively into the steelmaking process.[5–23] In particular, Jin[5,6] found that CO_2 gas injection into the steelmaking process, can remove the [C] in steel and achieve a smelting effect. Yi[7–14] carried out industrial tests of CO_2-O_2 mixed gas blown in basic oxygen furnace (BOF). The results of their study showed that the average rate of dust generation was reduced by 19.3 pct. Lv[15–17] found that, compared with blowing pure O_2 in a BOF, the dephosphorization rate was increased by 13.39 pct through CO_2 injection. Fruehan[18] studied the potential benefits of CO_2 or Ar injection for stirring in an electric arc furnace (EAF). Gu and Zhu[19,20] introduced a CO_2-Ar mixed gas into a 75t ladle furnace (LF) and found that the CO_2 does not affect the quality of the molten steel. However, there have been few researches on the effects of CO_2 captured from steel factories and injected during RH refining process in place of Ar gas.

The advantages of RH are the degassing and removal of inclusions utilizing a high vacuum and circulation flow. Owing to the use of a vacuum chamber, the RH process can avoid the reoxidation of molten steel from air and slag, and the stirring of RH can be quite strong.[24] This process can be used to achieve a large production capacity and high efficiency. In the course of CO_2 injected through snorkel nozzles under vacuum conditions in RH, CO_2 can be used to increase the stirring intensity by reacting with a small amount of [C]

BAOCHEN HAN and RONG ZHU are with the School of Metallurgical and Ecological Engineering, University of Science and Technology Beijing, No. 30, Xueyuan Road, Haidian District, Beijing 100083, China and also with the Beijing Key Laboratory of Research Center of Special Melting and Preparation of High-end Metal Materials, University of Science and Technology Beijing, No. 30, Xueyuan Road, Haidian District, Beijing 100083, China. Contact e-mail: zhurong_1201@126.com YIQIANG ZHU, RUNZAO LIU, WENHE WU, and GUANGSHENG WEI are with the School of Metallurgical and Ecological Engineering, University of Science and Technology Beijing, No. 30, Xueyuan Road, Haidian District, Beijing 100083, China. Contact e-mail: wgshsteel@126.com QIANG LI is with the Nanjing Iron and Steel Group Co., Ltd., Ning Steel Road, Liuhe District, Nanjing 210035, China

Manuscript submitted June 5, 2018.
Article published online September 21, 2018.

in molten steel.[7,25,26] Further research has determined that CO_2 can react with [Al] as gas bubbles rise in the up-snorkel.[27] Moreover, the proper [Al] content is critical to the quality of the steel produced.[28,29]

In this study, based on low-carbon molten steel with [C] of 0.05 to 0.20 pct and using FactSage 7.0 software, the selective oxidation sequence of [C] and [Al] with CO_2 was researched and analyzed under the RH refining temperature and vacuum degree. The concepts of a "carbon oxidation zone" and an "aluminum oxidation zone" were also proposed for the first time. Preliminary industrial trials were carried out to investigate the refining effect of molten steel with the introduction of CO_2 gas.

II. THERMODYNAMICS

A. *Gibbs Free Energy of the Reaction of CO_2 with [C], Fe, [Si], and [Al] in Steel*

By calculating the Gibbs free energy of the reactions, it can be determined whether the reactions between carbon dioxide and the elements in steel occur. Owing to the uncertain value of the CO partial pressure, the standard Gibbs free energy of the reactions between CO_2 and the elements in molten steel was calculated under refining conditions. Detailed calculation results of [C], Fe, [Si], and [Al] in steel were analyzed, and the results of which are shown in Table I. The extent of the chemical reactions can be estimated at equilibrium. This section mainly focuses on the degree of reactions of carbon dioxide gas with the elements in molten steel under thermodynamic equilibrium, and the influence on the refining process.

These four reactions can occur at the refining temperature, as shown in Table I, because the partial pressure of CO is close to zero before the reaction occurs. Moreover, the values of $\ln K^{\theta}$ indicate that CO_2 reacts more thoroughly with [Al] than [C], [Si], and Fe in molten steel. In the actual refining process, because little Fe reacts with CO_2, the reaction could be negligible.[11,30] However, CO_2 reacts more easily with [Al] than with [C], which may affect the refining effect and quality of the molten steel. Hence, it is necessary to study the conditions that contribute to the occurrence of the reaction of CO_2 with [C].

B. *Thermodynamics of Decarburization with CO_2 Injection in RH*

As described in Section II–A, CO_2 can react with [C] and [Al] at the steelmaking temperature. During actual production, the reaction of CO_2 with [Al] occurs more thoroughly than with [C]. However, CO_2 needs to react with [C] as much as possible, because the reaction of CO_2 with [Al] will increase the loss of aluminum, resulting in an increase in cost.

According to the principle of Le Chatelier, Reaction [1] is influenced from the bubble pressure in molten steel. In this section, assuming that CO_2 only reacts with [C] during the refining process of CO_2 gas injected into the RH up-snorkel, the favorable conditions of Reaction [1] are explored.

The reaction of CO_2 with [C] under vacuum condition is shown below:

$$[\mathrm{C}] + \mathrm{CO_2} = 2\mathrm{CO(g)} \uparrow \qquad [1]$$

$$\Delta_r G^{\Theta} = 137890 - 126.52\ \mathrm{T} \qquad [2]$$

$$K^{\Theta} = \frac{(p_{\mathrm{CO}}/P^{\Theta})^2}{a_{\mathrm{C}} \times p_{\mathrm{CO_2}}/P^{\Theta}} = \frac{(p_{\mathrm{CO}})^2}{[\mathrm{PctC}] \times f_{\mathrm{C}} \times P^{\Theta} \times (P^0 - p_{\mathrm{CO}})}, \qquad [3]$$

where $\Delta_r G^{\Theta}$, K^{Θ}, p_{CO}, $p_{\mathrm{CO_2}}$, P^{Θ}, P^0, a_{C}, f_{C}, and [pctC] are the standard Gibbs free energy, reaction equilibrium constant, pressure of CO and CO_2 in a bubble, standard atmospheric pressure, pressure inside bubble, activity, activity coefficient of carbon, and carbon content in molten steel, respectively.

$$p_{\mathrm{CO_2}} = P^0 - p_{\mathrm{CO}} \qquad [4]$$

At a temperature of 1873 K, the standard state of infinite dilute solution is taken, and at $f_{\mathrm{C}} = 1$, the following equation can be derived as follows:

$$[\mathrm{PctC}]^e = \frac{(p_{\mathrm{CO}})^2}{K^{\Theta} \times P^{\Theta} \times (P^0 - p_{\mathrm{CO}})}. \qquad [5]$$

Here, $[\mathrm{PctC}]^e$ is carbon content at equilibrium.

Because $\Delta_r G^{\Theta} = -RT \ln K^{\Theta}$, $K^{\Theta} = 579.86$ can be calculated at 1873 K. In addition, P^{Θ}can be set at 101,325 Pa. The relationship between carbon content and CO partial pressure in the bubbles is obtained as follows:

$$[\mathrm{PctC}]^{\mathrm{e}} = \frac{(p_{\mathrm{CO}})^2}{5.875 \times 10^7 \times (P^0 - p_{\mathrm{CO}})}. \qquad [6]$$

The vacuum pressure of RH can currently reach below 100 Pa, as can that of the bubbles. When setting $P^0 = 100$ Pa, Eq. [7] is expressed according to Eq. [6].

$$[\mathrm{PctC}]^{\mathrm{e}} = \frac{(p_{\mathrm{CO}})^2}{5.875 \times 10^7 \times (100 - p_{\mathrm{CO}})}. \qquad [7]$$

The curve of the relationship between the carbon content ([pctC]) and CO partial pressure is shown in Figure 1.

During the process of Reaction [1], with an increase in the CO partial pressure in a bubble, the partial pressure of CO_2 and the reaction rate gradually decrease. For reactions at equilibrium, the greater the CO partial

Table I. Standard Gibbs Free Energy of Reactions Between Elements and CO_2

Elements in Molten Steel	Reaction Equations	ΔG^{Θ}/J mol^{-1}	$\ln K^{\Theta} = -\frac{\Delta G^{\Theta}}{RT}$ (1873 K)
C	$[C] + CO_{2(g)} = 2CO_{(g)}$	$\Delta G^{\Theta} = 137890-126.52\ T$	6.363
Fe	$Fe(l) + CO_{2(g)} = (FeO) + 2CO_{(g)}$	$\Delta G^{\Theta} = 48980-40.62\ T$	1.740
Si	$1/2[Si] + CO_{2(g)} = 1/2(SiO_2) + CO_{(g)}$	$\Delta G^{\Theta} = -123970+20.59\ T$	5.484
Al	$2/3[Al] + CO_{2(g)} = 1/3(Al_2O_3) + CO_{(g)}$	$\Delta G^{\Theta} = -239370+41.44\ T$	10.387

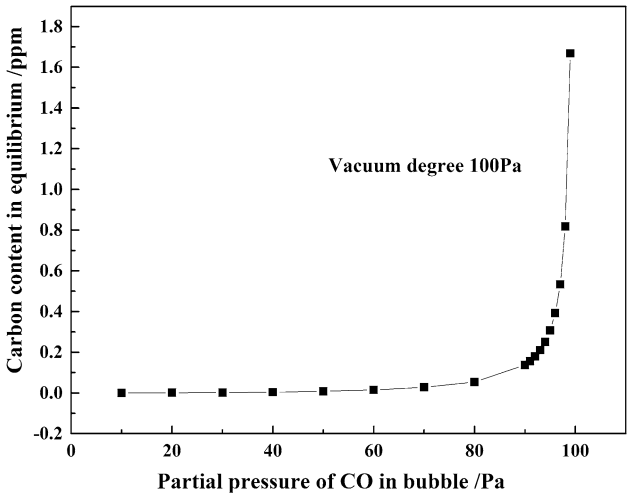

Fig. 1—Changes of carbon content at equilibrium as function of partial pressure of CO in bubble.

pressure is in the bubble, the greater the carbon content. From Figure 1, it can be observed that if CO_2 only reacts with [C], [pctC] could drop below 1.8 ppm under a vacuum degree of 100 Pa. This indicates that, as an RH lifting gas, CO_2 can react with [C] to enhance the RH stirring intensity, even refining low-carbon steel. To achieve a realistic level of production, the reaction between CO_2 and [Al] should be taken into account.

C. *Influence of Initial [Al] Content on Amount of Oxidation of [C] and [Al]*

FactSage 7.0 software was used to analyze the oxidation sequence of [C] and [Al] with CO_2 when refining low-carbon steel in RH. Only a few model parameters were introduced to reproduce the evolution of the [Al] and [C] contents in the steel based on industrial sampling data for the process conditions.[31,32] To simplify the calculation, the oxygen content in steel was set to under 10 ppm, which is the value after deep deoxidization of molten steel. The iron content in molten steel was set to 100 g during the calculation. The specific settings during the calculation are shown in Tables II and III.

The reaction mass of the elements is defined as the amount of elements oxidized through CO_2 injection, according to the reactions in Table I. In this section, the reaction masses of [C] and [Al] are calculated in molten steel with a certain carbon amount described. By changing the initial aluminum content in steel, the relationship between the reaction masses of [C], [Al], and the initial aluminum content can be obtained, as shown in Figure 2.

Table II. FactSage 7.0 Database Setting List

Option	Database Setting
Calculation mode	equilib
Database	FactPS, FToxide, FSstel
Solution module	FSstel-LIQU, FToxide-SLAGA
Compound module	gaseous phase: CO_2, CO, O_2 liquid steel phase: Fe, Al, O, C slag phase: Al_2O_3, FeO

Table III. FactSage 7.0 Menu List

Reactants and Final Conditions	Data
Fe	100 g
C	0.06 to 0.1 g
Al	Varied
O	0.001 g
CO_2	0.03954 g
Final conditions	bubble pressure 1000 Pa, temperature 1873 K

As Figure 2 indicates, the relationship between the reaction masses of [C] and [Al] varied with the difference in initial aluminum content during refining process. It can be seen from Figure 2 that, with an increase in the initial [Al] content, the amount of [Al] oxidized by CO_2 gradually increases at equilibrium, whereas the opposite is true for [C]. For a certain type of steel, the initial [Al] content is fixed, and thus the reaction masses of [C] and [Al] are fixed. The intersection of the two lines in Figure 2(a) means that, when refining steel with [pctC] = 0.07 and the initial [Al pct] = 0.0355, the reaction masses of [C] and [Al] at equilibrium are the same.

Figure 2 also indicates that there is a maximum value of the initial [Al] content, below which the [Al] will only slightly oxidize in molten steel. For example, when refining steel with [pctC] = 0.09, as shown in Figure 2(b), the [Al] in steel will only oxidize if the initial [pctAl] is less than 0.04. Hence, [Al pct] = 0.04 is the maximum value for [Al] when only slightly oxidized. Furthermore, the maximum value increases with an increase in [pctC].

The phenomenon of selective oxidation between [C] and [Al] by CO_2 bubbles entering the molten steel is mainly related to four factors, namely, the [C] content, [Al] content, bubble pressure, and temperature. The CO_2 reacts with [C] first when used to refine steel with

high [C] and low [Al] contents, and the opposite is true. According to Reaction [1] for CO_2 with [C], the volume of the CO_2-CO mixed gas increases compared with the original volume of the CO_2, which indicates an endothermic reaction. Therefore, decreasing the bubble pressure and increasing the temperature can promote the reaction of CO_2 with [C]. A reduction in temperature, however, would accelerate the reaction of CO_2 with [Al].

In certain types of steel, [pctC] and [pctAl] are at fixed values. Thus, only the effects of the bubble pressure and molten steel temperature on the selective oxidation were considered. During the FactSage software calculation, by setting the constants of [pctC], bubble pressure, and temperature, the authors found that the priority reaction of CO_2-[C] gradually changes into a CO_2-[Al] reaction. We defined this transition point as the "limiting aluminum content," which means the maximum [pctAl] at which the CO_2-[Al] does not react first.

Figure 3 shows the changes in limiting [Al] content with the increase in bubble pressure. It is clear that, the limiting [Al] content decreases sharply with an increase in the bubble pressure, the reason for which can be described as follows: With the increase in internal pressure of the bubbles, mainly due to the increase in CO, the CO_2-[C] reaction is restrained, which easily leads to a CO_2-[Al] reaction. At the same bubble pressure, the limiting [Al] content is positively correlated with the [C] content in steel.

Figure 4 shows that the limiting [Al] content changes with the increase in refining temperature. As indicated in Figure 4, the limiting [Al] content gradually increases with an increase in temperature. The CO_2-[Al] reaction is exothermic, and increasing the temperature inhibits the reaction from easily occurring. Furthermore, at the same temperature, the limiting [Al] content is also positively correlated with the [C] content in steel.

Under actual conditions, when CO_2 gas is injected into RH, the internal pressure of the bubbles gradually decreases to the vacuum degree as the bubbles rise in the up-snorkel. Based on the above analysis and conclusion drawn, a diagram of the [C] and [Al] oxidation rate in the up-snorkel is provided in Figure 5.

As shown in Figure 5, the distance between the molten steel surface in the vacuum chamber and the molten steel surface of the ladle is 1.45 m, and the pressure gradient is about 100 KPa. The internal pressure of the bubbles decreases as the bubbles rise from the nozzles to the molten steel surface in the vacuum chamber. According to the previous analysis, decreasing the pressure can promote the reaction rate of CO_2-[C]. Therefore, the [C] oxidation rate is gradually increased as the bubbles rise, whereas the opposite occurs for [Al]. We defined the upper part as the carbon

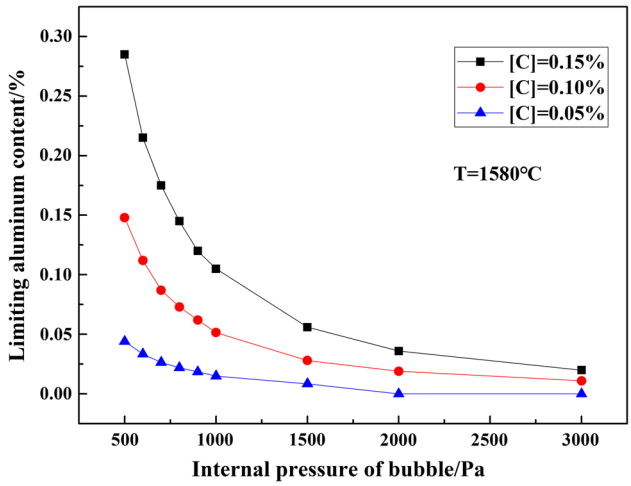

Fig. 3—Changes of limiting aluminum content as function of pressure in bubble.

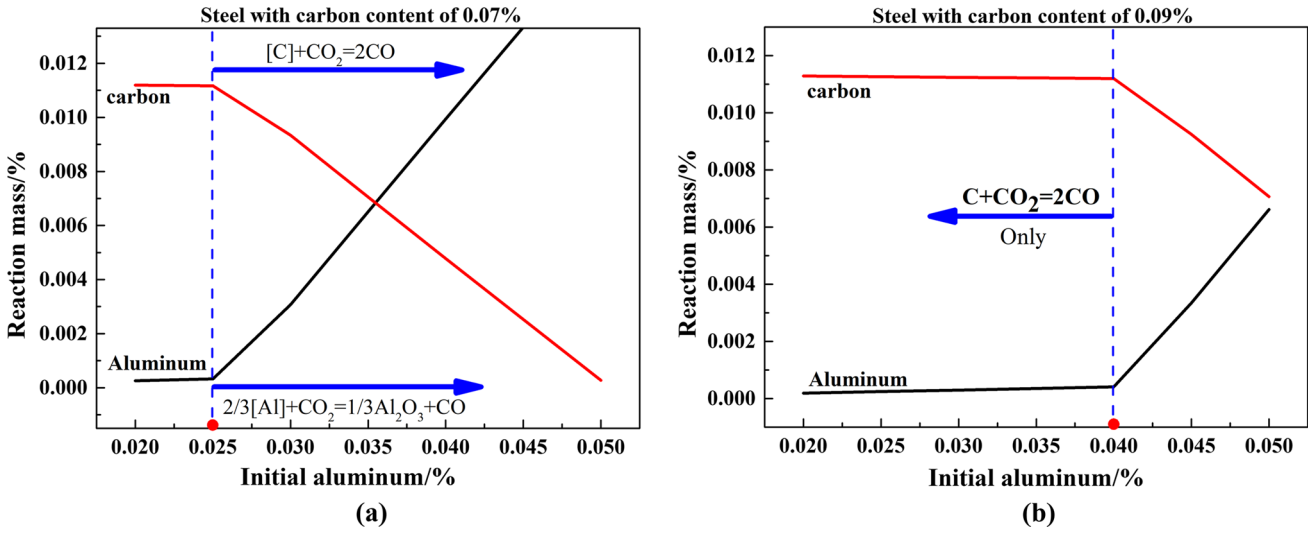

Fig. 2—(*a*) Reaction mass of [C] and [Al] as function of initial aluminum content with carbon content of 0.07 pct. (*b*) Reaction mass of [C] and [Al] as function of initial aluminum content with carbon content of 0.09 pct.

oxidation zone, as shown in Figure 5, where the reaction of CO_2 with [C] is faster than with [Al], and similarly, the lower part as the aluminum oxidation zone.

Based on the above analysis, the following three cases can be described:

(a) When the initial [Al] content is very high compared to the [C] content in steel, [Al] is oxidized much faster than [C] through the CO_2. Most of the CO_2 molecules react with [Al] as the CO_2 bubbles pass through the aluminum oxidation zone, and the CO_2-CO mixed gas in the bubbles continues to rise. The bubbles then arrive at the carbon oxidation zone; however, fewer CO_2 molecules in the bubbles can react with [C]. The entire process results in a large loss of aluminum and little decarburization before and after the refining process. Thus, this new process is not suitable for ultra-low-carbon steel.

(b) When the initial [Al] content is at the mid-level in steel, compared to case (a), the oxidation rate of [Al] decreases, whereas the oxidation rate of [C] increases. A portion of the CO_2 molecules react with [Al] and a small amount of [C] as the CO_2 bubbles pass through the aluminum oxidation zone, and the mixed CO_2-CO gas in the bubbles continues to rise. The bubbles then reach the carbon oxidation zone, and the remaining CO_2 molecules in the bubbles will react with [C] and a small portion of [Al]. Therefore, the entire process results in a partial aluminum loss and decarburization before and after the refining process.

(c) When the initial [Al] content is lower in steel, the entire process is opposite to that of case (a). Furthermore, the entire process achieves the purpose of decarburization and reduces the loss of aluminum.

In particular, if the original content of [Al] decreases or [C] increases, the carbon oxidation zone will enlarge, and the aluminum oxidation zone will decrease, as indicated with the black dotted line in Figure 5.

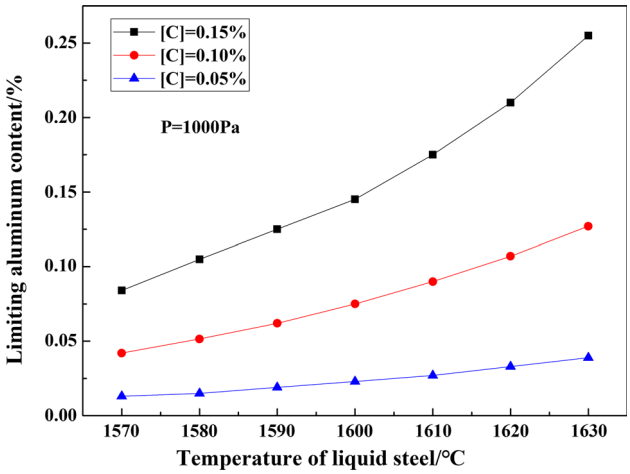

Fig. 4—Changes of limiting aluminum content as function of temperature of molten steel.

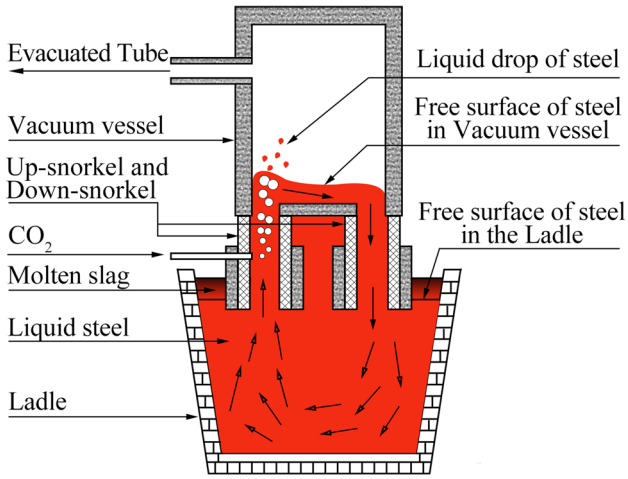

Fig. 6—Diagram of RH vacuum degasser.

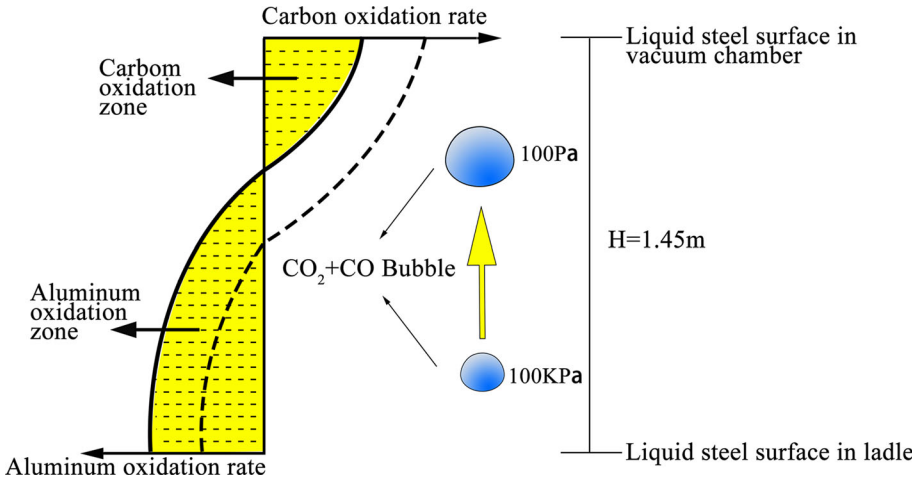

Fig. 5—Diagram of reaction between CO_2 and [C], [Al] in up-snorkel.

Table IV. Steel Composition of Ladle Pulling in RH (Mass Percent)

Component	C	Al	O	Si	Mn	P	S	Ni	Cr
Steel S	0.1280	0.0428	0.0040	0.2020	1.4314	0.0138	0.0041	0.0282	0.0400
Steel Q	0.1310	0.0210	0.0050	0.2436	1.2955	0.0147	0.0053	0.0186	0.0310

Table V. Gas Control Strategy and Test Scheme

Scheme	Steel	Dragging Gas	Gas Flow rate (Nm^3/h)	Refining Time (min)	Vacuum Degree (Pa)	Heats
1	S	Ar	100	18	67	10
2	S	CO_2	100	18	67	10
3	Q	CO_2	100	18	67	10
4	Q	CO_2	80	18	67	10
5	Q	Ar	120	18	67	10

III. INDUSTRIAL TRIALS

A. *Description of Industrial Trials*

Preliminary industrial trials were carried out to study the refining effect of molten steel with the introduction of CO_2 gas. As the CO_2 is injected from the up-snorkel into the RH as the power source of the molten steel circulation, its flowrate directly affects the circulation behavior of the molten steel.[33–37]

As shown in Figure 6, during the RH degassing, the molten steel is circulated between the vacuum vessel and ladle owing to the effect of CO_2 injected through the snorkel nozzles under vacuum conditions. It should be noted that no oxygen lance blowing, bottom blowing, or alloying occurs during this RH refining process. Before RH treatment, molten steel is deeply deoxidized by the additional aluminum treatment in the LF.

The trials involved two steel grades. The composition of the two steel grades and the test schemes are listed in Tables IV and V, respectively. It can be seen in Table IV that the initial [Al] content of steels S and Q is 0.0428 and 0.0210 pct, respectively. The five schemes shown in Table V, with ten heats for each scheme were designed to investigate the effects of the initial [Al] content and CO_2 gas on the RH refining process. Samples of molten steel were taken before and after the vacuum treatment. The [C] and [Al] contents in the steel samples were determined using a CS-2008 carbon/sulfur analyzer and Varian 715-ES acid-soluble aluminum analyzer. The hydrogen content in the molten steel was measured online by using a HYDRISHYDRIS immersion probe system.

The results before and after the RH refining indicate that no obvious changes in the silicon, manganese, nickel, chromium, or oxygen content in the steel occurred.

B. *Oxidation of [Al]*

Figure 7 shows the amount of aluminum loss per heat of industrial trials with the five schemes applied. The average aluminum loss of the five schemes differs because of the different steel species, gas types, and gas flow rates used. It can be seen that the average aluminum loss of scheme 1 through 5 is 40, 170, 50, 44, and 39 ppm, respectively. Owing to the weak oxidizing atmosphere in the vacuum chamber, aluminum loss occurs for each heat of scheme 1 and 5 with Ar gas injected into the up-snorkel. Nevertheless, the average aluminum loss of schemes 2, 3, and 4 with CO_2 gas injection is more than that of schemes 1 and 5, because CO_2 can react with [Al].

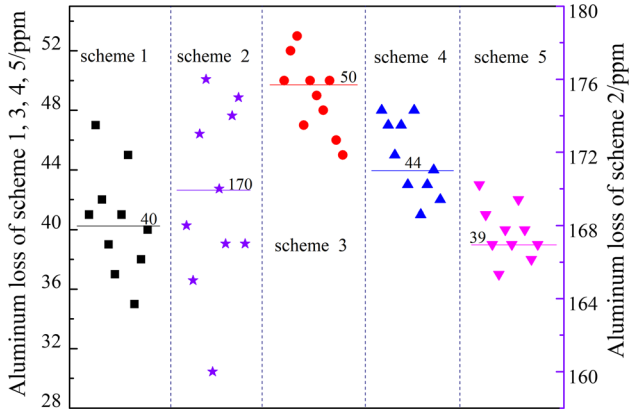

Fig. 7—Aluminum loss per heat of industrial trials.

Based on a comparative analysis using schemes 1 and 2, as indicated in Table IV and Figure 7, CO_2 injection causes 130 ppm more aluminum loss than Ar at the same gas flow rate during the refining process of steel S. The average aluminum loss of scheme 3 is 50 ppm, which is 120 ppm less than in scheme 2 at 170 ppm, which is due to the initial [Al] content in steel Q being 0.021 pct, which is lower than 0.0428 pct in steel S as compared to the initial carbon content. Because of the different CO_2 gas flow rates of 100 and 80 Nm^3/h, there is slight difference in the results of schemes 3 and 4, respectively. Therefore, it can be concluded that the initial [Al] content and gas type are the major factors affecting the loss of aluminum.

As shown in Figure 7, the results of scheme 2 can be explained through the following theory: The initial aluminum content in steel S is higher than in steel Q relative to the carbon content, and aluminum is oxidized much faster than carbon from the CO_2. Most of the CO_2 molecules react with aluminum as the CO_2 bubbles pass through the aluminum oxidation zone, and the mixed gas continues to rise. The bubbles then arrive at the carbon oxidation zone, and fewer CO_2 molecules in the bubbles can react with [C] (supplementary Figure S1). However, scheme 3 is opposite scheme 2. Thus, alloying can be adjusted to adapt to the RH refining process with CO_2 injection.

C. *Temperature Drop*

The temperature of steel is an important process index for RH refining, and was measured using a point-measurement method with thermal couples before and after the RH refining process. Figure 8 shows the average temperature drop of molten steel with five different schemes. As can be observed in Figure 8, a temperature drop occurs for each heat of the five schemes because of the circulation and physical cooling of the gas. The average temperature drop of schemes 1 through 5 is 40.7 °C, 39.3 °C, 42.7 °C, 41.5 °C, and 43 °C, respectively.

A comparative analysis of the temperature drop from schemes 1 through 5 was carried out. For schemes 1 and 2, the temperature drop of molten steel in scheme 1 is 1.4 °C greater than that in scheme 2, which is because the CO_2 injection in scheme 2 causes 130 ppm more aluminum loss than the Ar injection in scheme 1, as indicated in Figure 7, and moreover, the reaction of CO_2 with [Al] is exothermic. For scheme 3, more CO_2 molecules react with [C] than with [Al], and thus the temperature drop is greater than in scheme 2 owing to this endothermic reaction. Comparing the results of schemes 1 and 5, the larger Ar gas flow rate in scheme 5 creates a larger circulation flow rate and greater physical cooling effect of the gas, leading to a decrease of 43 °C. Above all, the CO_2 injection during the RH refining process will not cause a significant fluctuation in the temperature of the molten steel.

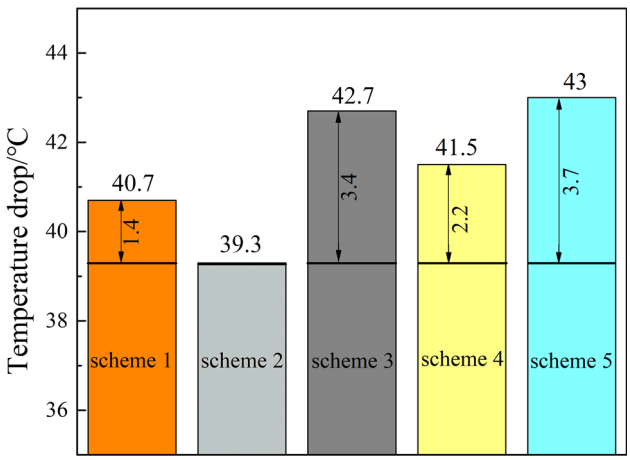

Fig. 8—Average temperature drop of molten steel.

D. *Dehydrogenation Efficiency*

The dehydrogenation effect is an important index reflecting the effect of the RH refining process, which is related to the circulation flow rate, vacuum degree, and number of bubbles.[38] Figure 9 shows the average dehydrogenation efficiency of schemes 1 through 5, namely, is 54.9, 57.1, 62.7, 59.4, and 60.8 pct, respectively.

As shown in Table V and Figure 9, the dehydrogenation ratio of scheme 5 is obviously 5.9 pct higher than in scheme 1, which can be explained by the following reasons: Owing to the larger Ar gas flow rate of scheme 5, a better dynamic degassing condition is provided, and the larger circulation flow rate accelerates the degassing of the molten steel. For schemes 2, 3, and 4, a larger volume of gas is generated by CO_2 reacting with [C] in molten steel, and thus the dehydrogenation ratio of schemes 2, 3, and 4 is higher than in scheme 1. In particular, the dehydrogenation ratio of scheme 3 is 7.8 pct higher than in scheme 1. It can be observed in Figure 9 that schemes 3 and 5 are the better test schemes. Therefore, it can be concluded that CO_2 injection during the RH refining process can achieve a better refining effect by adjusting the time and parameters of alloying for adaption to the RH refining process.

In the preliminary trials, low-carbon molten steel was used as a new process. Further trials will be carried out on other steel types to investigate the reactions of CO_2 with Si, Mn, and Ni alloys. In addition, the influence of this new process on the metallurgical effect will be studied.

IV. CONCLUSIONS

In the present study, the selective oxidation of [C] and [Al] with CO_2 was researched and calculated using FactSage software, and an aluminum oxidation zone and carbon oxidation zone were defined and discussed under different initial [Al] contents in molten steel. Industrial trials were preliminarily conducted to verify the above theory. Synthesizing the theoretical calculation and industrial trials, the following conclusions can be drawn.

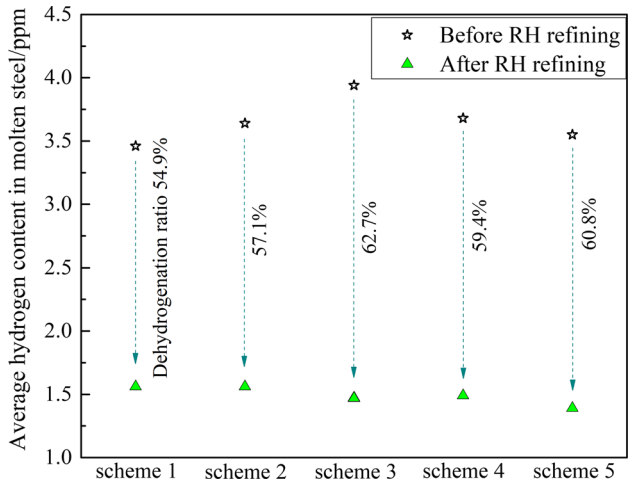

Fig. 9—Average dehydrogenation efficiency of each scheme.

(1) As an RH lifting gas, CO_2 can react with a small portion of [C], enhancing the RH stirring intensity. Moreover, CO_2 gas can be used to refine low-carbon steel in RH, and the end-point [C] content is determined based on the CO partial pressure and total amount of CO_2 injection.
(2) The initial [Al] content has a significant influence on the oxidation of [C] and [Al]. The lower the initial [Al] content is, the better the effect of decarburization with CO_2 injected during the RH refining process. For a certain content of [C] in steel, there is a maximum value of the initial [Al] content below which the [Al] will not be oxidized. Furthermore, the initial [Al] content is at least less than the limiting aluminum content when CO_2 is introduced during the RH refining process.
(3) As the CO_2 bubbles rise, the oxidation rate of [C] gradually increases, whereas the opposite occurs for [Al]. The initial contents of [C] and [Al] can affect the proportion of the carbon and aluminum oxidation zones, which means that the carbon oxidation zone will enlarge and the aluminum oxidation zone will become smaller if the original [Al] or [C] content decreases or increases, respectively.

By reducing the additive amount of aluminum alloy in the LF for controlling the initial [Al] content of molten steel, CO_2 injection will achieve a lower temperature drop of molten steel and a better refining effect than Ar injection during the RH degassing process, and thus the newly proposed process will not cause a significant loss of aluminum.

ACKNOWLEDGMENTS

Financial support by NSFC is gratefully acknowledged (Nos. 51334001, 51574021, and 51734003). The authors are also thankful to Nanjing Iron and Steel Group Co., Ltd. for support of industrial trials.

ELECTRONIC SUPPLEMENTARY MATERIAL

The online version of this article (https://doi.org/10.1007/s11663-018-1417-2) contains supplementary material, which is available to authorized users.

REFERENCES

1. K. Meijer, M. Denys, J. Lasar, J.P. Birat, G. Still, and B. Overmaat: *Ironmak. Steelmak.*, 2009, vol. 36, pp. 249–51.
2. M.A. Quader, S. Ahmed, S.Z. Dawal, and Y. Nukman: *Renew. Sustain. Energy Rev.*, 2016, vol. 55, pp. 537–49.
3. N.R. Neelameggham and R.G. Reddy: *TMS 2008 Annual Meeting*, Wiley, New Orleans, 2008, pp. 59–69.
4. T. Miwa and H. Okuda: *J. Jpn. Inst. Energy*, 2010, vol. 89, pp. 28–35.
5. R.J. Jin, R. Zhu, L.X. Feng, and Z.J. Yin: *J. Univ. Sci. Technol. Beijing*, 2007, vol. 29, pp. 77–80.
6. Z.J. Yin, R. Zhu, C. Yi, B.Y. Chen, C.R. Wang, and J.X. Ke: *Iron Steel*, 2009, vol. 44, pp. 92–94.
7. C. Yi, R. Zhu, B.Y. Chen, C.R. Wang, and J.X. Ke: *ISIJ Int.*, 2009, vol. 49, pp. 1694–99.
8. R. Zhu, X.R. Bi, M. Lv, R.Z. Liu, and X. Bao: *Adv. Mater. Res.*, 2011, vols. 284–286, pp. 1216–22.
9. C. Yi, R. Zhu, Z.J. Yin, N.N. Hou, B.Y. Chen, C.R. Wang, and J.X. Ke: *Chin. J. Process Eng.*, 2009, vol. 9, pp. 222–25.
10. X.J. Ning, Z.J. Yin, C. Yi, R. Zhu, and K. Dong: *Steelmaking*, 2009, vol. 25, pp. 32–34.
11. Z.Z. Li, R. Zhu, G.H. Ma, and X.L. Wang: *Ironmak. Steelmak.*, 2016, vol. 374, pp. 1–8.
12. R. Zhu, C. Yi, B.Y. Chen, C.R. Wang, and J.X. Ke: *Energy Metall. Ind.*, 2010, vol. 29, pp. 48–51.
13. X.R. Bi, R.Z. Liu, R. Zhu, and M. Lv: *Ind. Heat.*, 2010, vol. 39, pp. 13–16.
14. W. Zhang, Z.Z. Li, R. Zhu, and R.Z. Liu: *Ind. Heat.*, 2015, vol. 44, pp. 41–44.
15. M. Lv, R. Zhu, X.Y. Wei, H. Wang, and X.R. Bi: *Steel Res. Int.*, 2012, vol. 83, pp. 11–15.
16. M. Lv, R. Zhu, X.R. Bi, N. Wei, C.R. Wang, and J.X. Ke: *Iron Steel*, 2011, vol. 46, pp. 31–35.
17. M. Lv, R. Zhu, X.R. Bi, and T.C. Lin: *J. Univ. Sci. Technol. Beijing*, 2011, vol. 33, pp. 126–30.
18. R.J. Fruehan: in *Electric Furnace Conference Proceedings*, 1988, pp. 259–66.
19. Y.L. Gu, H.J. Wang, R. Zhu, J. Wang, M. Lv, and H. Wang: *Steel Res. Int.*, 2014, vol. 85, pp. 589–98.
20. K. Dong, R. Zhu, R.Z. Liu, H. Wang, and C.F. Zhou: *J. Univ. Sci. Technol. Beijing*, 2014, vol. 36, pp. 226–29.
21. G.S. Wei, R. Zhu, T. Cheng, K. Dong, L.Z. Yang, T.P. Tang, and X.T. Wu: *ISIJ Int.*, 2018, vol. 58, pp. 842–51.
22. G.S. Wei, R. Zhu, X.T. Wu, K. Dong, L.Z. Yang, and R.Z. Liu: *JOM*, 2018, vol. 70, pp. 969–76.
23. G.S. Wei, R. Zhu, X.T. Wu, L.Z. Yang, K. Dong, T. Cheng, and T.P. Tang: *Metall. Mater. Trans. B*, 2018, vol. 49B, pp. 1405–20.
24. X.H. Wang, L.F. Zhang, Q.L. Shan, and X.F. Liu: *Steel Res. Int.*, 2013, vol. 84, pp. 473–89.
25. J.R. Paules: in *70th Steelmaking Conference Proceedings* (Pittsburgh), 1987.
26. M.X. Guo, X.W. Chen, Q.A. Xiao, L. Duan, and Y.S. Liu: *J. Univ. Sci. Technol. Beijing*, 1991, vol. 5, pp. 410–16.
27. Y.Q. Zhu, R. Zhu, and X.L. Wang: *Ind. Heat.*, 2017, vol. 46, pp. 7–8.
28. S.H. Chen, X.H. Wang, X.F. He, M. Jiang, and F.X. Huang: *Iron Steel*, 2011, vol. 46, pp. 42–47.
29. C.L. Lu, J.W. Li, and C.Q. Li: *Foundry*, 2017, vol. 66, pp. 277–81.
30. G. Wei, Z.T. Li, Z.L. Li, Q.J. Gao, and F.M. Shen: *J. Iron Steel Res. Int.*, 2016, vol. 23, pp. 98–102.
31. M.K. Cho, M.A. Van Ende, T.H. Eun, and I.H. Jung: *J. Eur. Ceram. Soc.*, 2012, vol. 32, pp. 1503–17.
32. C.W. Bale, E. Bélisle, P. Chartrand, S.A. Decterov, G. Eriksson, K. Hack, I.H. Jung, Y.B. Kang, J. Melancon, A.D. Pelton, C. Robelin, and S. Peterson: *Calphad*, 2009, vol. 33, pp. 295–311.
33. C.W. Li, G.G. Cheng, X.H. Wang, G.S. Zhu, and A.M. Cui: *J. Iron Steel Res. Int.*, 2012, vol. 19, pp. 23–28.
34. G.J. Chen and S.P. He: *Vacuum*, 2016, vol. 130, pp. 48–55.
35. P.H. Li, Q.J. Wu, W.H. Hu, and J.S. Ye: *J. Iron Steel Res. Int.*, 2015, vol. 22, pp. 63–67.
36. K.F. Feng, A. Liu, K.J. Dai, S. Feng, J. Ma, J.Y. Xie, B. Wang, Y.W. Yu, and J.Y. Zhang: *Powder Technol.*, 2017, vol. 314, pp. 649–59.
37. J. Zhou, Z. Qin, B. Zhang, Q.C. Peng, S.T. Qiu, and Y. Gan: *J. Iron Steel Res. Int.*, 2013, vol. 20, pp. 40–44.
38. J.H. Qi, J.G. Zheng, G.Y. Chen, P.F. Zhang, T.M. Ye, and J.J. Fei: *Eng. Sci. J.*, 2016, vol. 38, pp. 125–28.